Infrared Multiphoton Dissociation of Acetone in a Molecular Beam†

Cindy L. Berrie,* Cheryl A. Longfellow,‡ Arthur G. Suits,§ and Yuan T. Lee||

Lawrence Berkeley National Laboratory, Chemical Sciences Division, and Department of Chemistry, University of California, Berkeley, California 94720

Received: October 3, 2000

The infrared multiphoton dissociation of acetone has been studied for the first time under the collisionless conditions of a molecular beam. A single carbon−carbon bond rupture channel resulting in the formation of an acetyl radical and a methyl radical is the only primary channel observed. The translational energy distribution for this channel peaks near zero with an average translational energy release of only 2.0 kcal/mol as expected for a reaction with no exit barrier. Significant secondary decomposition of the acetyl radical to carbon monoxide and methyl radical is also observed. The translation energy distribution determined for this channel is peaked well away from zero with an average energy release of 6.1 kcal/mol indicating that it proceeds on a potential energy surface with a barrier, consistent with previous UV experiments. No molecular elimination pathways are observed under the conditions of these experiments.

1. Introduction

By determination of the primary products of a unimolecular reaction as well as the translational and internal energy distributions of the products, a great deal can be learned about the dynamics of the dissociation event. For example, a simple bond rupture reaction will have a translational energy distribution which is peaked near zero, with only a small amount of energy deposited in the relative motion of the two fragments.[1] On the other hand, a decomposition channel which occurs through a concerted elimination pathway with a substantial barrier will have a large fraction of the available energy channeled into translational energy of the fragments as they repel each other down the barrier resulting in a translational energy distribution peaked well away from zero.[2−5]

By careful analysis of photofragment translational spectroscopy data, it is possible to extract quantities such as the heats of formation of the products and the relative activation energies for competing channels in the decomposition process.[5,6]

Many experiments have been performed to determine the kinetic parameters (activation energy and Arrhenius *A* factor) for thermal dissociation processes (see for example refs 7 and 8). These experiments are necessarily performed under conditions where collisions are used to heat the molecules of interest. Under these conditions, the primary products of the decomposition are often difficult to determine as they can (and do) undergo secondary reactions before they are detected. One technique that has often been used to overcome this difficulty is infrared multiphoton decomposition (IRMPD). In IRMPD, the molecules are vibrationally heated by successive absorption of IR photons (usually from a CO_2 laser). The absorbed energy is rapidly randomized by intramolecular vibrational energy redistribution.

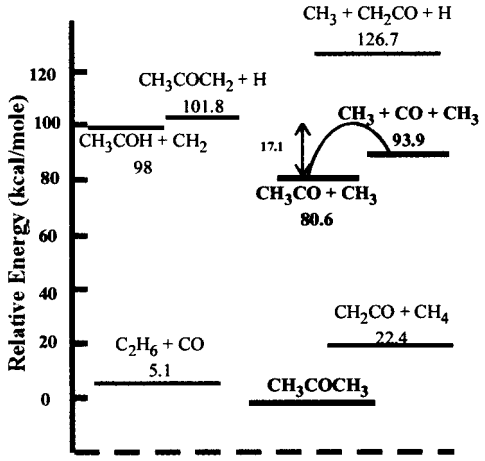

Figure 1. Schematic diagram of the energetics of acetone decomposition. The heats of formation of all products were from Benson,[28] and the barrier height for acetyl dissociation was taken from ref 6.

This results in molecules with energy distributions which are nearly identical to thermal distributions.[9] It has been shown in a large number of experiments that the primary products following infrared excitation are identical to those of a thermal decomposition.[10] However, because the IRMPD technique relies on absorption of photons for heating and not on collisions, it can be easily incorporated in a molecular beam apparatus where the decomposition can take place under collisionless conditions. This allows for unambiguous determination of the primary products as well as the determination of their translational energy distributions through photofragment translational spectroscopy.[10]

The photolysis[11−23] and pyrolysis[7,8,25−27] of acetone have been studied extensively. A schematic diagram of the relative energies of several possible reaction pathways is presented in Figure 1. The heats of formation for acetone, CH_3CO, CH_2CO, CH_3, CH_2, CH_3COH, CH_4, and CO were all obtained from ref 28. The barrier shown for the acetyl radical decomposition is taken from ref 6. The primary step in the UV photodissociation of acetone on the first excited (S_1) state is a simple carbon−carbon bond

† Part of the special issue "William H. Miller Festschrift".

* Corresponding author. Permanent address: Department of Chemistry, University of Kansas, Lawrence, KS 66045.

‡ Present address: Department of Chemistry, Philadelphia University, Philadelphia, PA 19144-5497.

§ Present address: Department of Chemistry, SUNY at Stony Brook, Stony Brook, NY 11794-3400.

|| Present address: Institute of Atomic and Molecular Sciences, Academia Sinica, Taipei, Taiwan, ROC.

10.1021/jp003620v CCC: $20.00
Published on Web 01/31/2001

rupture through reaction 1.[15]

$$CH_3COCH_3 \rightarrow CH_3 + CH_3CO \quad (1)$$

If the acetyl fragment is formed with sufficient internal energy, secondary decomposition to a methyl radical and CO can occur as shown in reaction 2.[6,20]

$$CH_3CO \rightarrow CH_3 + CO \quad (2)$$

There has been a large amount of work done to determine the time scale for the two carbon−carbon bond breaking steps in cases where the products are two methyl radicals and CO.[14,16,19−23] Specifically, many groups have attempted to answer the question of whether the decomposition is stepwise or concerted. Currently, the general consensus is that the decomposition proceeds stepwise as described above, through an acetyl intermediate. This picture of acetone photolysis is supported by recent theoretical calculations.[24]

Several possible molecular elimination pathways have also been investigated, one example being the formation of methane and ketene through reaction 3.

$$CH_3COCH_3 \rightarrow CH_2CO + CH_4 \quad (3)$$

Hydrogen atom loss through reaction 4 and ethane formation through reaction 5 are two other possible channels:

$$CH_3COCH_3 \rightarrow CH_3COCH_2 + H \quad (4)$$

$$CH_3COCH_3 \rightarrow C_2H_6 + CO \quad (5)$$

These channels (reactions 4 and 5) have been determined to be less than 1.5% of the dissociation yield in the UV photolysis of acetone.[20]

On the other hand, the most abundant products in the pyrolysis of acetone have been determined to be methane and ketene.[12,27] These are thought to be secondary reaction products from an abstraction reaction following the primary cleavage of the carbon−carbon bond in reaction 1.[27] Thus the thermal dissociation of acetone is a prime example of a system where the primary products are difficult to determine owing to collisions which can result in secondary reactions. Two IRMPD studies of acetone under bulb conditions have been reported in the literature where the final products are analyzed,[29,30] but again the primary products are not easily determined because of collisions and secondary reactions. In the first of these experiments,[29] methane and ethane are observed as significant reaction products. In the second experiment, ethylene, acetylene, hydrogen, and propane are observed in addition to methane and ethane. The only two IRMPD studies performed to date leave open the question of what are the primary pathways in the thermal decomposition of acetone, since they were performed under conditions where secondary reactions dominate the products observed. To our knowledge, this paper presents the first study of the IRMPD of acetone under collisionless conditions, providing direct measurements of the primary reaction pathways as well as the translational energy distributions of the resulting fragments.

Since the most abundant products of the pyrolysis of acetone are methane and ketene and these products are very stable, the possibility exists that these products can be formed through a molecular elimination channel. This would involve a four-center transition state where a hydrogen atom is transferred from one methyl group to the other. Such elimination channels are not unprecedented. In the decomposition of acetic acid, two molecular elimination channels have been observed,[5] a decarboxylation channel resulting in CO_2 and methane and a dehydration channel to form water and ketene. In addition, the molecular elimination of ethanol and ethylene from diethyl ether IRMPD has been observed.[31] Recently, the molecular elimination of HCl from chemically activated acetyl chloride has also been postulated.[32] These reactions must all proceed through similar tight transition states. Both thermal decomposition and IRMPD occur predominately through the lowest energy pathway available, but in cases where the activation energies for two or more channels are similar, there can be a competition between the two and both may be observed.

2. Experimental Section

These experiments were conducted using a rotating source molecular beam machine described in detail elsewhere.[33] Briefly, a mixture of acetone or acetone-d_6 in helium was generated by passing ∼240 Torr of helium through a bubbler maintained at −20 °C. This resulted in a ∼4% mixture. For these experiments, the mixture was expanded through a 0.005 in. nozzle held at a temperature of ∼260 °C to eliminate the formation of clusters in the beam. The resulting beam typically had a velocity of 1760 m/s with a fwhm spread of 16% for the acetone-d_6 and a velocity of 1835 m/s with a fwhm spread of 16% for the normal acetone. The beam velocity and velocity spread were measured by time of flight using a spinning slotted wheel.[34]

The molecular beam was crossed at the interaction region with the output from a Lumonics TEA 840 CO_2 laser operating on the P(12) line of the 9.6 μm band at 1054 cm^{-1} for the acetone-d_6 and the R(20) line of the 9.6 μm band at 1082 cm^{-1} for the normal acetone. The products resulting from the IRMPD process travel 36.7 cm to the detector where they are ionized using an electron impact ionizer, mass selected with a quadrupole mass filter, and counted using a Daly type ion counter. The signal is collected in 2 μs bins by a multichannel scaler triggered with the laser pulse. In this manner, the time-of-flight spectra are collected at all masses where product signal is observed. The angle between the source and detector can be changed by rotating the source around the interaction region while leaving the detector fixed. The resulting time-of-flight spectra are analyzed using a forward convolution fitting procedure described previously[35] to obtain the product center of mass translational energy distributions.

3. Results

We present here in detail only the results for the acetone-d_6 experiments because the signal-to-noise ratio is better at many of the product masses for the deuterated case. The results for the normal acetone experiments show no qualitative differences. For the acetone-d_6 experiments, laser dependent signal was detected at the following mass-to-charge ratios: m/e 46 (CD_3CO^+), m/e 44 (CD_2CO^+), m/e 42 ($CDCO^+$), m/e 30 ($C_2D_3^+$), m/e 28 (CO^+), m/e 26 (C_2D^+), m/e 18 (CD_3^+), m/e 16 (CD_2^+), and m/e 14 (CD^+). The signals in the case of normal acetone corresponded to the same product species, with the mass of hydrogen replacing that for deuterium. The signal was measured at source to detector angles of 10, 15, 20, 30, and 40° at two different laser fluences, ∼38 and ∼57 J/cm^2. The deuterated acetone data presented here were all taken at a laser fluence of ∼57 J/cm^2.

The signal observed in the experiments conducted on normal acetone was much weaker than that observed from the acetone-d_6 which is consistent with the results of the only other IRMPD

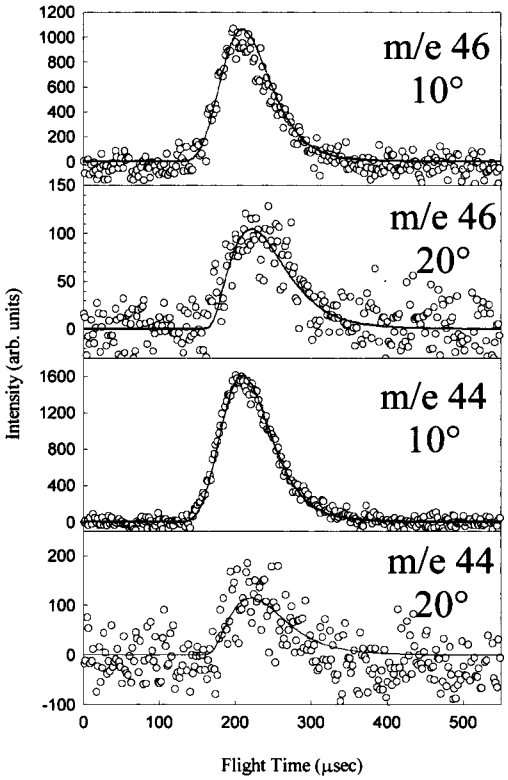

Figure 2. Time-of-flight spectra obtained at *m*/*e* 46 (CD_3CO^+) and *m*/*e* 44 (CD_2CO^+) at source to detector angles of 10 and 20°. The circles are the experimental data, while the solid line is a fit to the data using the translational energy distribution shown in Figure 3.

studies of this molecule.[29,30] In the range of wavelengths of the CO_2 laser, deuterated acetone absorbs more strongly than normal acetone. Typically, the signal at *m*/*e* 15 (CH_3^+) at a fluence of ~65 J/cm^2 is about a factor of 7 weaker than the signal observed at *m*/*e* 18 (CD_3^+) in the deuterated acetone experiments conducted at a laser fluence of ~57 J/cm^2. It should be noted, however, that neither of these compounds absorbs strongly in this wavelength region. In the normal acetone experiments, the signal nearly disappears when the fluence is dropped to ~40 J/cm^2. However, in the case of acetone-d_6, signal is still observed at a fluence of 38 J/cm^2, again indicating the stronger absorption of the deuterated acetone.

The highest mass-to-charge ratio at which laser dependent signal was observed was *m*/*e* 46 (CD_3CO^+). No signal was observed at *m*/*e* 62 which would have indicated the occurrence of the hydrogen atom loss channel, reaction 4. However, this channel would be very difficult to detect given our experimental setup, since the heavy fragment would not recoil far from the molecular beam. High background count rates at angles closer than 10° off the molecular beam axis make measurements there very difficult. Therefore, while we think this channel is unlikely, given its significantly higher energy (see Figure 1), it cannot be completely ruled out.

The time-of-flight signal observed at *m*/*e* 46 is shown in Figure 2 at source to detector angles of 10 and 20°. The open circles are the experimental data, and the solid lines are the fits to the data calculated from the translational energy distribution shown in Figure 3, assuming that the signal is the result of the simple carbon−carbon bond rupture channel shown in reaction 1.

Also shown in Figure 2 is the signal measured at *m*/*e* 44 (CD_2CO^+). Note that the signal measured at this mass is identical to that observed at *m*/*e* 46. The fit to the data at *m*/*e* 44 assumes that the signal at this mass results only from dissociatively ionized acetyl radical generated through reaction 1. The fact that there is no additional component in the *m*/*e* 44 spectrum (CD_2CO^+) is direct evidence that reaction 3 is not occurring in this system.

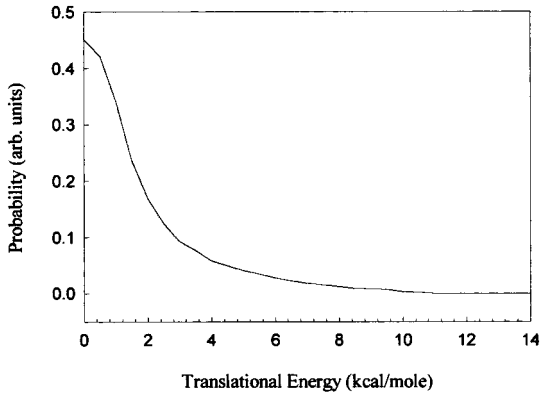

Figure 3. Translational energy distribution for primary carbon−carbon bond cleavage (reaction 1).

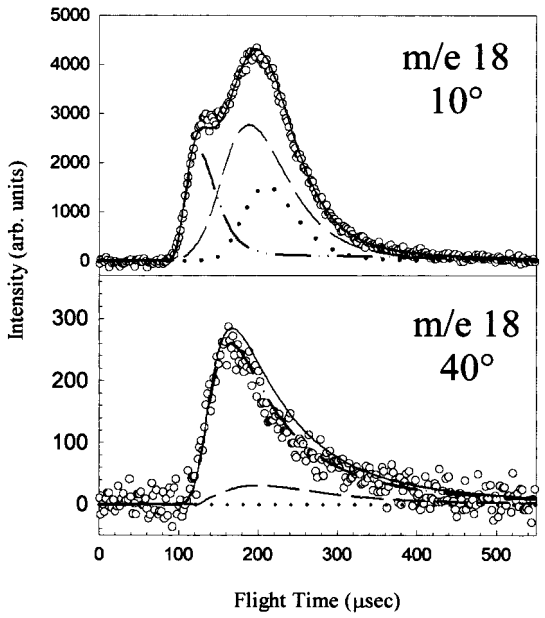

Figure 4. Time-of-flight spectra measured at *m*/*e* 18 at 10 and 40° from the molecular beam axis. The solid line is the overall fit to the data, the dotted line is dissociatively ionized acetyl radical, the dashed line is the primary methyl fragment, and the dashed−dotted line is the secondary methyl fragment.

Additional evidence that reaction 3 is not occurring is the absence of signal at *m*/*e* 20 (CD_4^+) (not shown). Even after signal averaging for ~300,000 laser shots, the time-of-flight spectrum showed no indication of this product. (Incidentally, if this channel did exist, it would be easier to detect in the deuterated acetone, since there is very little background in our mass spectrometer at this mass, as opposed to the case of normal methane at *m*/*e* 16.)

The signal observed at *m*/*e* 18 at 10 and 40° is shown in Figure 4. The open circles are the experimental data, and the lines represent different components of the fit to the data. The dotted line is the contribution of dissociatively ionized acetyl radical, the dashed line is the methyl radical resulting from reaction 1, the dashed−dotted line is a contribution due to secondary decomposition of the acetyl radical through reaction 2, and the solid line is the overall fit to the data. The signal due to the primary methyl radical is fit with the same translational

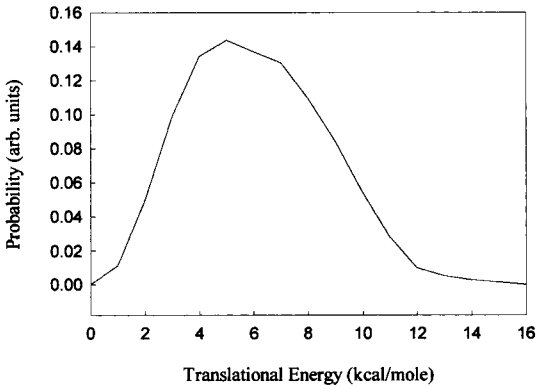

Figure 5. Translational energy distribution for secondary decomposition of the acetyl radical (reaction 2).

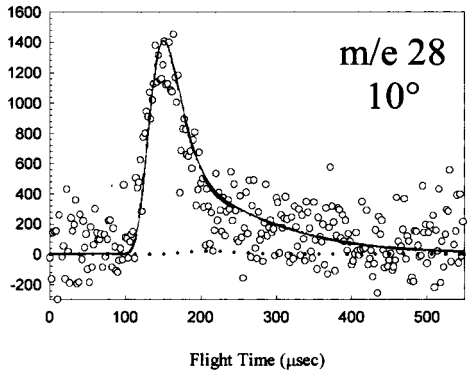

Figure 6. Time-of-flight spectrum measured at *m*/*e* 28 at 10° from the molecular beam axis. The circles are the experimental data, the dotted line is a possible contribution from dissociatively ionized acetyl, the dashed−dotted line is the CO formed from secondary dissociation of acetyl (reaction 2), and the solid line is the overall fit to the data.

energy distribution shown in Figure 3 that was used to fit the acetyl spectrum, proving that these two fragments are indeed momentum matched partners resulting from the same dissociation event.

The translational energy distribution used to fit the signal due to the secondary decomposition of the acetyl radical is shown in Figure 5. The partner fragment in this secondary decomposition is CO, and the time-of-flight spectrum measured at *m*/*e* 28 is shown in Figure 6. The circles are the experimental data, the dashed line represents a possible small contribution due to dissociatively ionized acetyl radical, the dashed−dotted line is CO from the secondary decomposition of the acetyl radical, and the solid line is the overall fit to the data. It should be noted that these data can be fit equally well without including a contribution from dissociatively ionized acetyl; this fit is only included to illustrate that there could possibly be a small contribution and that the majority of the signal could not be fit assuming it was coming from dissociatively ionized acetyl. The majority of the time-of-flight signal obtained at this mass is much too fast (appearing at short times) to be fit in that way. The observation of fast translationally hot CO is consistent with the assignment of the short time signal in the methyl spectrum to secondary dissociation of acetyl to give CO and CD_3. A comparison of the yields of primary methyl and primary acetyl products gives a rough estimate of 40 ± 20% for the fraction of acetyl radicals that undergo secondary dissociation under these experimental conditions. The fits to the data are reasonably insensitive to the exact shape of the secondary angular distribution, as long as the distribution is kept forward−backward symmetric.

The signals observed at the other mass-to-charge ratios can all be explained by assuming that they result from dissociative ionization of one of the products already discussed. Thus, they reveal no new reaction channels. In particular, no new contribution to the signal at *m*/*e* 16 is observed which could indicate the loss of CD_2 to form acetaldehyde, reaction 6.

$$CH_3COCH_3 \rightarrow CH_3CHO + CH_2 \qquad (6)$$

Additionally, there was no signal observed at the mass of ethane which would indicate the molecular elimination of ethane.

4. Discussion

4.1. Carbon−Carbon Bond Rupture. As discussed in section 2, the signal observed can be explained as being due to the primary reaction of acetone through simple carbon−carbon bond rupture to give acetyl and methyl radicals, followed by the secondary decomposition of the acetyl radical to form methyl radical and carbon monoxide. The primary translational energy distribution shown in Figure 3 is peaked near zero and extends to only 5−6 kcal/mol, with an average energy in translation of only 2.0 kcal/mol. This is typical of a simple bond rupture reaction which occurs with no barrier to reaction beyond the endothermicity of the reaction.

4.2. Secondary Decomposition of Acetyl Radicals. The translational energy distribution for the secondary decomposition of acetyl shown in Figure 5 of the acetyl radical is peaked well away from zero with an average energy in translation of 6.1 kcal/mol. This is nearly identical to the translational energy distribution obtained for the secondary decomposition of acetyl following UV excitation of acetone to the S_1 state.[20] This is a clear indication that the secondary decomposition of acetyl radical is occurring on the same potential energy surface in both the UV experiments and the present IRMPD experiment. The fact that this distribution is peaked away from zero indicates that there is a significant barrier to the secondary decomposition of acetyl radical. In fact, this barrier has previously been estimated as 17.1 kcal/mol.[6,20,21] While in the case of the UV experiments the energy is deposited in the molecule by absorption of a single photon with a well-defined energy, in IRMPD the acetone molecules each absorb a different number of photons, generating a range of internal energies which make extracting an accurate barrier quite difficult. In addition, the acetyl radical can also absorb more photons as long as it is born in the interaction region during the laser pulse, which opens up the possibility that the dissociation of the acetyl radical is a result of subsequent absorption and not hot acetyl radicals formed in the primary dissociation step. More likely, there is a contribution from both effects. Since there is almost certainly a large difference in the internal energy of the acetyl radical in these two experiments, the similarity of the translational energy distributions indicates that the translational energy release is controlled in large part by the recoil of the fragments down the repulsive part of the potential beyond the barrier to dissociation.

4.3. Normal Acetone. Figure 7 shows the *m*/*e* 15 (CH_3^+) time of flight spectrum from the IRMPD of normal acetone. The contributions to the signal in this spectrum are the same as those in the deuterated methyl spectrum shown in Figure 4. Notice that in this case the fast signal, which arises from secondary decomposition of the acetyl radical, is significantly smaller than in the case of the deuterated acetone. (The normal acetone data were collected at a fluence of 65 J/cm^2 while the fluence for the data shown for deuterated acetone was 57 J/cm^2.) This could mean that the deuterated acetone is being pumped

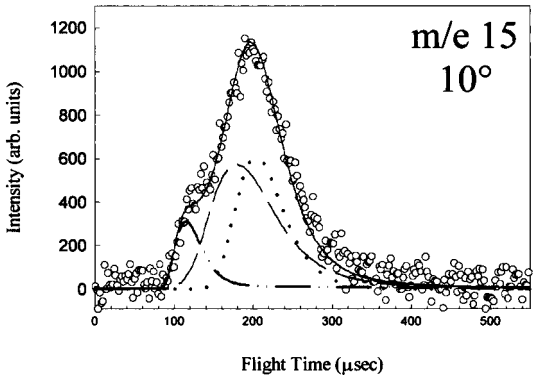

Figure 7. Time-of-flight spectrum measured at *m*/*e* 15 in the IRMPD of normal acetone at 10° from the beam axis. The contributions are identical to those in Figure 4.

to a higher excitation level before dissociating than the normal acetone due to the greater absorption cross section, or it could be that the nascent deuterated acetyl radical absorbs additional photons more easily than the normal acetyl radical. Our results cannot distinguish between these two possibilities. The translational energy distributions used to fit the data are identical to the ones used to fit the data for the deuterated case, within experimental error. The time-of-flight spectra at all other masses in the normal acetone experiment can also be fit equally well using the same translational energy distributions as the deuterated acetone case.

4.4. Lack of Molecular Elimination Channels. As discussed in the Introduction, the IRMPD process commonly proceeds through the channel with the lowest activation energy. However, if two or more channels have similar activation energies, they can compete and multiple pathways can be observed. The fact that we do not observe the elimination of either methane or ethane, even though these pathways give rise to very stable products, suggests that the barriers to their formation significantly exceed that of the simple bond rupture channel. This puts a lower limit on the activation energies for the formation of these products; however, they could be much higher. The Arrhenius preexponential factors for the molecular elimination pathways are expected to be significantly lower than those for simple bond rupture since they would have to proceed through a tight, constrained transition state. They would thus compete less effectively if their barriers were near that for the simple bond rupture channel, but they should still be observable.

The molecular elimination of methane involving a hydrogen atom migration has been observed in the case of IRMPD of acetic acid.[5] In this case, another channel involving hydrogen atom transfer resulting in the formation of water and ketene was also observed. Both of these channels were observed under the same experimental conditions indicating that the barriers are similar, and in this case they were determined to be 62−72.5 kcal/mol. Setser et al. have also recently observed the molecular elimination of HCl from acetyl chloride (which again involves a hydrogen atom transfer) after chemical activation.[32] However, this molecular elimination channel is not observed in the UV dissociation of acetyl chloride.[6] Another case where a hydrogen migration gives rise to a molecular elimination channel is the IRMPD of diethyl ether. In this system, the formation of ethanol and ethylene results from hydrogen transfer from carbon to oxygen through a four center transition state.[31] Interestingly, another molecular elimination channel involving a hydrogen atom transfer in a four center transition state to give ethane and acetaldehyde was not observed, even though these products are more stable. Clearly, the observation of molecular elimination channels involving hydrogen migration in systems similar to acetone is not unprecedented. Thus, it is interesting that we do not see either of these molecular elimination channels in the IRMPD of acetone. To our knowledge, there are no theoretical estimates of the activation energies for the molecular elimination channels to give ethane or methane from acetone.

4.5. Comparison with Previous Results. As stated in the Introduction, the most abundant products in the thermal dissociation of acetone are methane and ketene.[12,27] Clearly, this is completely different from the result observed in the present experiment, in which a single primary carbon−carbon bond rupture channel is observed. The methane and ketene observed in the pyrolysis experiments are thought to arise from a methyl radical formed in the primary dissociation event extracting a hydrogen from another acetone molecule to give methane and acetonyl.[27] The acetonyl radical later decomposes to give ketene and another methyl radical, which can continue the cycle. This is illustrated by the series of reactions shown in reactions 7−9. Only the essential steps are shown here. The full reaction scheme proposed by Herzfeld is presented in both refs 8 and 27.

$$CH_3COCH_3 \rightarrow CH_3 + CH_3CO \quad (7)$$

$$CH_3 + CH_3COCH_3 \rightarrow CH_4 + CH_2COCH_3 \quad (8)$$

$$CH_2COCH_3 \rightarrow CH_2CO + CH_3 \quad (9)$$

Notice that the simple carbon−carbon bond rupture channel which is the first step in this scheme is the one observed in the present IRMPD experiment. The formation of methane and ketene occurs in secondary reaction steps involving collisions which do not occur in our experiments. Consistent with the explanation of the pyrolysis results, the methane and ketene observed cannot be the result of a molecular elimination reaction in a single step through reaction 3 but rather are the result of secondary reactions, since they are not observed under collisionless conditions.

The previous IRMPD studies of acetone[29,30] were performed in a gas cell where collisions cannot be ignored. One experiment shows results which are consistent with the mechanism presented above for pyrolysis in which they observe methane and ethane as significant products. The second experiment[30] reports acetylene, propane, ethylene, and hydrogen among the products in addition to ethane and methane. Clearly, these complex product distributions are the result of secondary reactions that occur following collisions. The results presented here provide unambiguous evidence for a single primary dissociation pathway involving carbon−carbon bond rupture in the "thermal" dissociation of acetone.

5. Conclusions

We report the first measurements of the infrared multiphoton dissociation of acetone and perdeuterated acetone under the collisionless conditions of a molecular beam. A single primary reaction channel involving simple carbon−carbon bond rupture through reaction 1 has been observed. The translational energy distribution determined for this channel is peaked near zero with an average energy of only 2.0 kcal/mol. This is consistent with a reaction proceeding with no barrier beyond the endothermicity of the reaction. Significant secondary dissociation of the acetyl radical is also observed resulting in the formation of CO and CH_3 (CD_3) radicals. The translational energy distribution for this channel is peaked well away from zero with an average translational energy release of 6.1 kcal/mol, suggesting dissociation on a potential energy surface with an exit barrier. This

is similar to the acetyl radical secondary dissociation observed in the UV photodissociation experiments. We observe no evidence for any other primary reaction pathways, including methane and ethane elimination under the present experimental conditions. The product distributions observed in both the previous thermal dissociation experiments and IRMPD experiments were clearly the result of secondary reactions, while the present experiments allowed clear determination of the primary reaction pathway.

References and Notes

(1) Sudbø, Aa. S.; Schulz, P. A.; Grant, E. R.; Shen, Y. R.; Lee, Y. T. *J. Chem. Phys*. **1979**, *70*, 912.

(2) Huisken, F.; Krajnovich, D.; Zhang, Z.; Shen, Y. R.; Lee, Y. T. *J. Phys. Chem*. **1983**, *78*, 3806.

(3) Sudbø, Aa.; Schulz, P. A.; Shen, Y. R.; Lee, Y. T. *J. Chem. Phys*. **1978**, *69*, 2312.

(4) Krajnovich, D.; Huisken, F.; Zhang, Z.; Lee, Y. T. *J. Chem. Phys*. **1982**, *77*, 5977.

(5) Longfellow, C. A.; Lee, Y. T. *J. Phys. Chem*. **1995**, *99*, 15532.

(6) North, S. W.; Blank, D. A.; Lee, Y. T. *Chem. Phys. Lett*. **1994**, *224*, 38.

(7) McNesby, J. R.; Davis, T. W.; Gordon, A. S. *J. Am. Chem. Soc*. **1954**, *76*, 823. McNesby, J. R.; Gordon, A. S. *J. Am. Chem. Soc*. **1954**, *76*, 4196.

(8) Rice, F. O.; Herzfeld, K. F. *J. Am. Chem. Soc.* **1934**, *56*, 284.

(9) Grant, E. R.; Schulz, P. A.; Sudbø, Aa. S.; Y. R. Shen, Y. R.; Lee, Y. T. *Phys. Rev. Lett*. **1978**, *40*, 115.

(10) Schulz, P. A.; Sudbø, Aa. S.; Krajnovich, D. J.; Kwok, H. S.; Shen, Y. R.; Lee, Y. T. *Annu. Rev. Phys. Chem*. **1979**, *30*, 379. Sudbø, A. S.; Schulz, P. A.; Shen, Y. R.; Lee Y. T. In *Multiple-Photon Excitation and Dissociation of Polyatomic Molecules*; Cantrell, C. D., Ed.; Springer-Verlag: Berlin, 1986.

(11) Cundall R. B.; Davies, A. S. *Prog. React. Kinet.* **1967**, *4*, 149.

(12) Bérces, T. In *Comprehensive Chemical Kinetics, Volume 5: Decomposition and Isomerization of Organic Compounds*; Bamford, C. H., Tipper, C. F. H., Eds.; Elsevier: Amsterdam, 1972.

(13) Hancock, G.; Wilson, K. R. In *Proceedings of the IVth International Symposium on Molecular Beams*; Cannes, France, 1973.

(14) Kroger, P. M.; Riley, S. J. *J. Chem. Phys*. **1977**, *67*, 4483.

(15) Lee, E. K. C. *Adv. Photochem*. **1980**, *12*, 1.

(16) Donaldson, D. J.; Leone, S. R. *J. Chem. Phys*. **1986**, *85*, 817. Woodbridge, E. L.; Fletcher, T. R.; Leone, S. R. *J. Phys. Chem*. **1988**, *92*, 5387.

(17) Lightfoot, P. D.; Kirwan, S. P.; Pilling, M. J. *J. Phys. Chem*. **1988**, *92*, 4938.

(18) Trentelman, K. A.; Kable, S. H.; Moss, D. B.; Houston, P. L. *J. Chem. Phys*. **1989**, *91*, 7498.

(19) Hall, G. E.; Vanden Bout, D.; Sears, T. J. *J. Chem. Phys*. **1991**, *94*, 4182. Hall, G. E.; Metzler, H. W.; Muckerman, J. T.; Preses, J. M.; Weston, R. E., Jr. *J. Chem. Phys*. **1995**, *102*, 6660.

(20) North, S. W.; Blank, D. A.; Gezelter, J. D.; Longfellow, C. A.; Lee, Y. T. *J. Chem. Phys*. **1995**, *102*, 4447.

(21) Kim, S. K.; Pedersen, S.; Zewail, A. H. *J. Chem. Phys*. **1995**, *103*, 477.

(22) Owrutsky, J. C.; Baronavski, A. P. *J. Chem. Phys*. **1998**, *108*, 6652. Owrutsky, J. C.; Baronavski, A. P. *J. Chem. Phys*. **1999**, *110*, 11206.

(23) Buzza, S. A.; Snyder, E. M.; Castleman, A. W. *J. Chem. Phys*. **1996**, *104*, 5040. Zhong, Q.; Poth, L.; Castleman, A. W. *J. Chem. Phys*. **1999**, *110*, 192.

(24) Liu, D.; Fang, W.-H.; Fu, X.-Y. *Chem. Phys. Lett.* **2000**, *325*, 86.

(25) Szwarc, M.; Taylor, J. W. *J. Chem. Phys*. **1955**, *23*, 2310.

(26) Clark, D.; Pritchard, H. O. *J. Chem. Soc*. **1956**, 2136.

(27) Mousavipour, S. H.; Pacey, P. D. *J. Phys. Chem*. **1996**, *100*, 3573.

(28) Benson, S. W. *Thermochemical Kinetics*; John Wiley & Sons: New York, 1976.

(29) McNesby, J. R.; Scanland, C. *Chem. Phys. Lett*. **1979**, *66*, 303.

(30) Braun, W.; McNesby, J. R. *J. Phys. Chem*. **1980**, *84*, 2521.

(31) Butler, L. J.; Buss, R. J.; Brudzynski, R. J.; Lee, Y. T. *J. Phys. Chem*. **1983**, *87*, 5106.

(32) Srivatsava, A.; Arunan, E.; Manke, G., II; Setser, D. W.; Sumathi, R. *J. Phys. Chem*. **1998**, *102*, 6412. Maricq, M.; Ball, I. C.; Straccia, A. M.; Szente, J. J. *Int. J. Chem. Kinet*. **1997**, *29*, 421.

(33) Wodtke, A. M.; Lee, Y. T. *J. Phys. Chem*. **1985**, *89*, 4744.

(34) See for example: Balko, B. A. Ph.D. Thesis, University of California, Berkeley, CA, 1991.

(35) Myers, J. D. Ph.D. Thesis, University of California, Berkeley, CA, 1993. Wodtke, A. M. Ph.D. Thesis, University of California, Berkeley, CA, 1986. Zhao, X. Ph.D. Thesis, University of California, Berkeley, CA, 1988.